Effective corrosion inhibition of mild steel in acidic medium using inexpensive kermes natural dye: experimental and quantum chemical study

Nobl F. El Boraei, Shimaa Abdel Halim and Magdy A.M. Ibrahim
Department of Chemistry, Ain Shams University, Cairo, Egypt

Abstract

Purpose – The purpose of this paper is to test the Natural Kermes dye (NKD) as a cheap and stable corrosion inhibitor for mild steel in 1.0 M HCl and its adsorption mechanism on the steel surface.

Design/methodology/approach – The inhibition action of NKD was studied using AC impedance, potentiodynamic polarization, scanning electron microscope (SEM) and UV-visible spectra techniques complemented with quantum study.

Findings – Here, the authors show that addition of NKD inhibits effectively the corrosion of steel in HCl solution via its adsorption on the steel surface. The inhibition efficiency of NKD increases with increase in its concentration and decreases with temperature. Potentiodynamic results revealed that NKD acts as a mixed–type inhibitor. Thermodynamic parameters for corrosion and adsorption process were obtained from the experimental data. Moreover, the experimental inhibition efficiencies were correlated with the electronic properties of NKD using density functional theory.

Originality/value – To the best of the authors' knowledge, this is the first report showing the effect of NKD on the corrosion inhibition of steel.

Keywords Corrosion, Mild steel, A.C. impedance, Kermes dye, Quantum study

Paper type Research paper

1. Introduction

Mineral acids, particularly HCl, are used in industrial processes such as acid cleaning, acid pickling, acid descaling and oil well acidizing (Ulaeto *et al.*, 2012). Inhibitors are usually used in these processes to control metal attack and acid consumption. Most of the acid inhibitors potentially used are organic compounds containing N-, S- and/or O atoms. These organic compounds can adsorb on the metal surface, blocking the active sites and therefore reduce the corrosion rate. Nowadays, non-toxicity should be taken as an important issue in selecting a suitable corrosion inhibitor. Unfortunately, many of the existing organic/inorganic corrosion inhibitors contain heavy metals and organic phosphates (Sekine *et al.*, 1988). The search for non-toxic and efficient corrosion inhibitors is on the increase demand (Matad *et al.*, 2014). Recently, several studies have been reported on the use of organic dyes as corrosion inhibitors (Oguzie, 2004; Oguzie *et al.*, 2004a, 2004b, 2006).

The objective of this work is to investigate the effect of NKD on the corrosion behavior of steel in 1.0 M HCl solution using A.C. impedance, potentiodynamic polarization techniques complemented with quantum chemical study. Effects of inhibitor concentration and temperature on the corrosion inhibition were fully investigated and discussed. To the best of our knowledge, this is the first report showing the effect of Natural Kermes dye (NKD) on the corrosion inhibition of steel.

2. Experimental details

2.1 Materials and aggressive solution

The mild steel specimen, with composition (Wt.%) Fe 99.09, C 0.17, Mn 0.70 and P 0.04, was used in the present study. Prior to corrosion test, steel specimen was mechanically polished with 1000 and 2000 series of emery papers, washed with double distilled water and with acetone. NKD is a brilliant red dye which is extracted from the shell of the female insects, which huddle immobile in clusters on the wood. The advantage in using NKD is not only its cheapness and its easily solubility in water at room temperature but also its color stability. Its uses have been documented in ancient Egypt when this color was known as the King's red and treasured as a painter's pigment. The molecular structure of the NKD is shown in Scheme 1.

The aggressive solution of 1.0 M HCl was prepared by diluting 36 per cent HCl with double distilled water. Various

The current issue and full text archive of this journal is available on Emerald Insight at: **www.emeraldinsight.com/0003-5599.htm**

Anti-Corrosion Methods and Materials
65/6 (2018) 626–636

[DOI 10.1108/ACMM-04-2018-1927]

Received 29 April 2018
Accepted 19 July 2018

Scheme 1 Structure of NKD

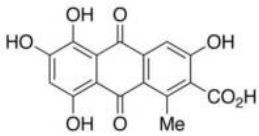

concentrations of NKD ($5 \times 10^{-5} - 5 \times 10^{-3}$ M) were prepared in 1.0 M HCl.

2.2 Electrochemical measurements

The measurements were done using Interface 1000 Gamry Instrument Potentiostat/Galvanostat/*ZRA*. The electrochemical cell consists of three electrode assembly; in which the working electrode was the steel, the reference electrode was Ag/AgCl and Pt electrode was the counter electrode. The electrochemical tests have performed in aerated solutions. Prior to measurements, the working electrode was immersed in 1.0 M HCl in absence and presence of NKD for 30 min. All impendence measurements were performed under a potentiodynamic condition from 100 KHz to 0.01 Hz with amplitude of 5 mV peak-to-peak. The potentiodynamic curves were recorded in the potential range of −1000 to 500 mV at a scan rate of 5 mVs^{-1}.

2.3 Computational method

Calculations have been performed using Khon-Sham's density functional theory (DFT) method subjected to the gradient-corrected hybrid density functional B3LYP method (Becke, 1993). This function is a combination of the Becke's three parameters non-local exchange potential with the non-local correlation functional of Lee *et al.* (1988). For each structure, a full geometry optimization was performed using this function (Lee *et al.*, 1988) and the 6-311G (p,d) bases set (Stefanov *et al.*, 2003) as implemented by Gaussian 09 package (Frisch *et al.*, 2009). All geometries were visualized either using GaussView 5.0.9 (Dennington *et al.*, 2009) or Chemcraft 1.6 software packages. No symmetry constrains were applied during the geometry optimization. The geometry of the adsorbed inhibitor on the electrode was initially guessed by semi-empirical calculation using p.m.6 Hamiltonian method (Stewart, 2007) using quadratic convergent self-consistent Field procedure (Bacskay, 1981).

2.4 Surface morphology

The surface morphology of mild steel in absence and presence of NKD inhibitor was evaluated using scanning electron microscopy (SEM) model (Shimadzu supper- scan SSX- 550).

2.5 UV-visible spectra

The absorption spectra of the NKD solutions in the presence and the absence of steel specimens were measured by UV-visible spectrometer (UV-1601PC, Shimadzu). UV spectra were obtained using glass cell with a light length of 1.0 cm.

3. Results and discussion

3.1 A.C. impedance

Impedance measurements of the steel electrode at its open circuit potential after 30 min of immersion in 1.0 M HCl solution in the absence and presence of various NKD concentrations were performed over the frequency range from 100 kHz to 10 mHz at 298 K. The impedance data are represented as shown in Figures 1 and 2 by both Nyquist and Bode plots, respectively. In Nyquist plot, the impedance spectra exhibit a single capacitive loop at high frequencies (HF) both in uninhibited and inhibited solutions. The capacitive loop at HF is due to the charge transfer of the corrosion process and double layer behavior. From Nyquist plot, it is obvious that the capacitive loops are not perfect semicircle which could be referred to inhomogeneous and roughness of the metal surface (Lebrini *et al.*, 2007). Furthermore, the capacitive loop

Figure 1 Nyquist plot for steel electrode in 1.0 M HC1 without and with different concentrations of NKD

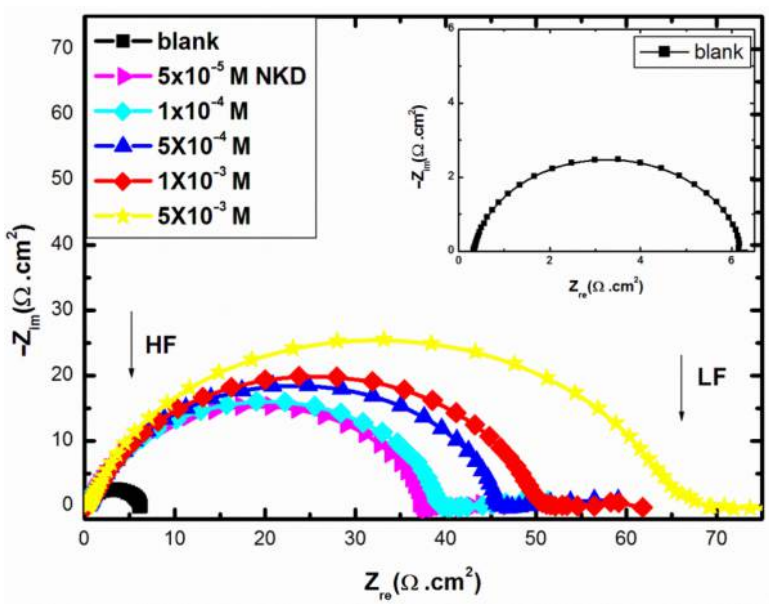

Figure 2 Bode plots for steel electrode in 1.0 M HC1 in absence and presence of different concentration of NKD

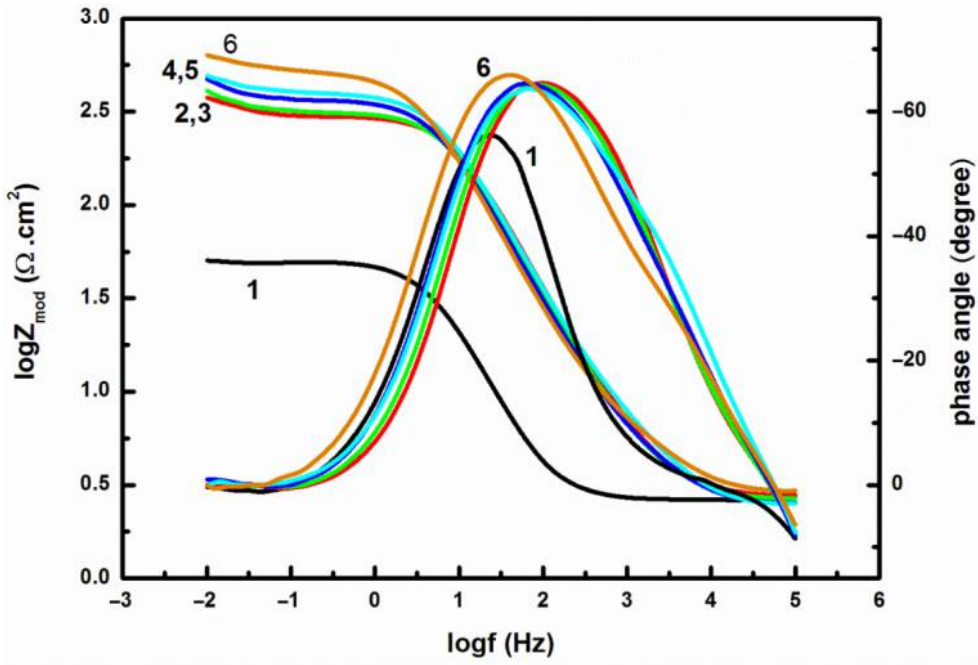

Notes: [1] blank; [2]5 × 10−5M; [3]1 × 10−4M; [4] 5 × 10−4M; [5] 1 × 10−3M; [6] 5 × 10−3M

diameter in the presence of NKD is larger than in its absence and increases with NKD concentration. This means that NKD acts as an excellent corrosion inhibitor for mild steel in 1.0 M HCl. On the other hand, Bode plot explore the presence of two phase maximums, one at HF and the second at low frequency, the former is due to C_{dl} (double layer capacitance) and the latter is controlled by film adsorption and desorption (Yan *et al.*, 2008). The impedance data are analyzed using the circuit shown in Figure 3. This circuit fits well our experimental data. As shown in Figure 3, the intersection of the capacitive loop with the real axis presents the ohmic resistances of the corrosion product films and the solution enclosed between the working electrode and the reference electrode, R_s (Quraishi and Rawat, 2002). The charge-transfer resistance R_{ct} whose value is a measure of electron transfers across the surface is inversely proportional to corrosion rate (Abdel-Gabar *et al.*, 2006). The constant phase element (CPE) is substituted for the capacitive element instead of a pure double layer capacitor to give a more accurate fit (Macdonald and Johanson, 1987). The impedance of a CPE is described in equation (1):

Figure 3 Equivalent circuits used to fit the impedance data

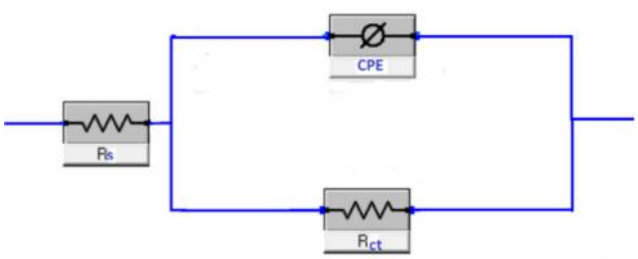

$$Z_{CPE} = \frac{1}{Y_0(j\omega)^n} \quad (1)$$

where Y_0 is the magnitude of the CPE, j is an imaginary number, ω is the angular frequency at which the imaginary component of the impedance reaches its maximum values and n is the deviation parameter of the CPE: $-1 \leq n \leq 1$. The values of the interfacial capacitance C_{dl} can be calculated from CPE parameter values Y_0 and n using equations (2) or (3) (Hsu and Mansfel, 2001):

$$C_{dl} = Y_0(\omega_{max})^{n-1} \quad (2)$$

$$C_{dl} = \frac{1}{R_{ct} \times \omega_{max}} \quad (3)$$

where, $\omega_{max} = 2\pi f_{max}$, f_{max} is the frequency at which the imaginary part of the impedance has a maximum.

The inhibition efficiency, *IE%*, of the tested inhibitor was calculated from the R_{ct} values at different concentrations using equation (4) (Abd El-Maksoud and Hassan, 2007):

$$IE\% = \left(1 - \frac{1/R_{ct(inh)}}{1/R_{ct(uninh)}}\right) \times 100 \quad (4)$$

where $R_{ct\ (uninh)}$ and $R_{ct\ (inh)}$ are the values of the charge transfer resistance without and with inhibitor, respectively. The values of the electrochemical parameters R_s, R_{ct}, via impedance fitting as well as the calculated parameters C_{dl} and *IE%* are gathered in Table I. The results indicate that the inhibition efficiency increased from 84.2 to 91.1 per cent with increasing the concentration of NKD from 5×10^{-5} to 5×10^{-3} M.

Table I Electrochemical parameters calculated from EIS measurements of the mild steel electrode in 1.0 M HCl in the absence and presence of different concentrations of NKD at 298K

C_{inh} (M)	R_s (Ω)	R_{ct} (Ω)	C_{dl} ($\mu F cm^{-2}$)	IE %
0.0	2.64	46.9	340.42	–
5×10^{-5}	2.80	313.4	127.47	84.2
1×10^{-4}	2.71	332.0	64.49	85.0
5×10^{-4}	2.6	389.5	60.88	87.1
1×10^{-3}	2.52	427.1	58.70	88.5
5×10^{-3}	3.09	561.6	43.62	91.10

Inspection of the data in Table I clearly shows that R_{ct} increases enormously, whereas C_{dl} decreases with the concentration of NKD. A large R_{ct} is associated with a slowly corroding system (Ashassi-Sorkhabi and Asghari, 2008). In addition, improved inhibitor protection is associated with a decrease in the metal capacitance. The reduce in C_{dl}, which originated from a decrease in the local dielectric constant and/or an increase in the thickness of the electrical double layer, suggested that NKD acted via adsorption at the metal/solution interface (Musa *et al.*, 2009). The decrease in C_{dl} also could be attributed to the adsorption of the inhibitor molecules forming a protective adsorption layer (Abdel-Gabar *et al.*, 2006).

3.2 Potentiodynamic polarization measurements

Figure 4 shows the potentiodynamic curves of mild steel in 1.0 M HCl without and with various concentrations of NKD. The polarization curves show similar features in the absence and presence of the inhibitor suggesting that the inhibitor retards mild steel corrosion by adsorption and blocking the active sites on the steel surface, without changing the corrosion mechanism (Olasunkanmi *et al.*, 2015). Moreover, the presence of NKD causes a decrease in both the anodic and cathodic current densities, i.e. decrease the corrosion rate. A lower corrosion current value for inhibitor solutions implies that the rate of electrochemical reactions was reduced due to the formation of a barrier layer over the steel surface by inhibitor molecules. The potentiodynamic parameters such as the corrosion current density (j_{corr}), the corrosion potential (E_{corr}), anodic (β_a) and cathodic (β_c) Tafel slopes and *IE%* are listed in Table II. The *IE%* values were calculated from j_{corr} values using the following equation (Hleli *et al.*, 2003):

$$IE\% = \left(1 - \frac{j_{corr(inh)}}{j_{corr(uninh)}}\right) \times 100 \quad (5)$$

where $j_{corr\ (uninh)}$ and $j_{corr\ (inh)}$ are the corrosion current densities in absence and presence of inhibitor, respectively. Table II shows the decrease in j_{corr} with increasing concentration of NKD but increased with temperature. The inhibitor can be regarded as anodic or cathodic – type inhibitor when the shift in E_{corr} in the presence of the inhibitor, is larger than 85 mV (Liu *et al.*, 2009). In the present study, the shift in E_{corr} lies between 37 and 62 mV (less than 85 mV) implying that the studied NKD is a mixed-type inhibitor, by inhibiting both the hydrogen reduction and the steel dissolution (Sorkhabi *et al.*, 2005). The results indicate that the *IE%* increased from 90.4 to 96.1 per cent with increasing the concentration of NKD from 5×10^{-5} to 5×10^{-3} M.

On the other hand, the *IE%* decreased proportionally with temperature. Such behavior can be explained by desorption of some adsorbed inhibitor molecules with rising the solution temperature (Wang, 2012).

3.3 Adsorption isotherms

Several adsorption isotherms were tested for the adsorption behavior of the studied NKD. The Langmuir adsorption isotherm was found to provide the best fit of the adsorption behavior of NKD at the steel/solution interface. The plot of C_{inh}/θ versus C_{inh} yields straight line (Figure 5) with R^2 = 0.999. This suggest that NKD in the present study obeyed the Langmuir

Figure 4 Potentiodynamic curves for steel corrosion in 1.0 M HCl without and with various concentrations of NKD

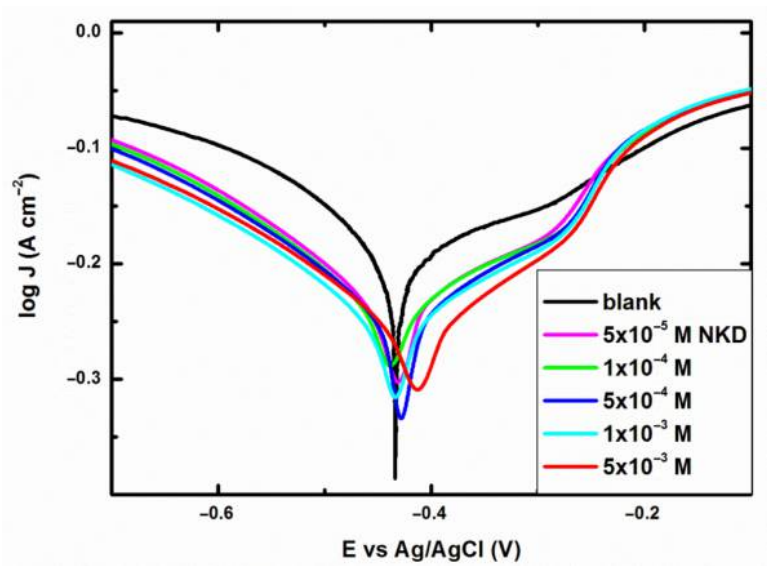

Table II Potentiodynamic polarization parameters for mild steel in 1.0 M HCl with different concentrations of NKD at various temperatures

Temp. K	C_{inh} M	j_{corr} Acm^{-2}	$^{-}E_{corr}$ V	β_a $Vdec^{-1}$	$-\beta_c$ $Vdec^{-1}$	θ	IE%
298	0.0	7.1×10^{-3}	0.476	0.278	0.237	–	–
298	5×10^{-5}	6.8×10^{-4}	0.439	0.269	0.218	0.904	90.4
298	1×10^{-4}	6.1×10^{-4}	0.438	0.257	0.204	0.914	91.4
298	5×10^{-4}	4.7×10^{-4}	0.429	0.245	0.201	0.934	93.4
298	1×10^{-3}	3.4×10^{-4}	0.425	0.224	0.199	0.952	95.2
298	5×10^{-3}	2.8×10^{-4}	0.414	0.21	0.190	0.961	96.1
308	0.0	7.6×10^{-3}	0.437	0.495	0.501	–	–
308	5×10^{-5}	2.9×10^{-3}	0.431	0.487	0.497	0.623	61.8
318	0.0	7.9×10^{-3}	0.441	0.505	0.515	–	–
318	5×10^{-5}	3.1×10^{-3}	0.439	0.496	0.502	0.609	60.8
328	0.0	0.015	0.422	0.521	0.531	–	–
328	5×10^{-5}	11.6×10^{-3}	0.399	0.510	0.522	0.230	22.7
338	0.0	0.019	0.392	0.544	0.552	–	–
338	5×10^{-5}	17.0×10^{-3}	0.389	0.515	0.531	0.105	10.5

Figure 5 Langmuir adsorption plot for steel in 1.0 M HCl containing different concentrations of NKD

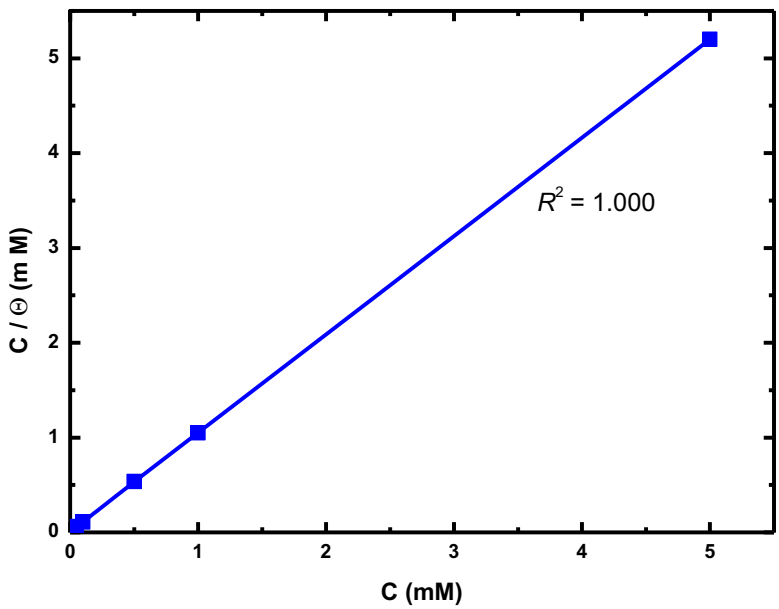

adsorption isotherm which is given as (Machnikova *et al.*, 2008):

$$C_{inh}/\theta = 1/K_{ads} + C_{inh} \quad (6)$$

where C_{inh} is the inhibitor concentration, θ is the degree of surface coverage (θ = (IE%/100), K_{ads} is the equilibrium constant of the adsorption process. On the other hand, the standard free energy of adsorption, $\Delta G°_{ads}$ at 298K was calculated from the following equation (Machnikova *et al.*, 2008):

$$\Delta G°_{ads} = -RT \ln (55.5\ K_{ads}) \quad (7)$$

where 55.5 is the molar concentration of water, R is the universal gas constant and T is the temperature in Kelvin. The negative value of $\Delta G°_{ads}$ means that the adsorption of NKD molecules on mild steel surface is a spontaneous process, while the high value of K_{ads} (1.89 × 105) indicates the strong interaction of the inhibitor molecule onto the steel surface (Yurt *et al.*, 2005). It is well-known that values of $\Delta G°_{ads}$ equals −20 kJ mol^{-1} or less are compatible with physisorption, while those which are more negative than −40 kJ mol^{-1} involve chemisorption (Saliyan and Adhikari, 2008). In the present study, the calculated $\Delta G°_{ads}$ value of the NKD is −39.98 kJ mol^{-1} (Table III), indicating that the adsorption of NKD on the steel surface is mainly chemisorption.

3.4 Effect of temperature

The effect of temperature on the *IE%* of NKD, polarization experiments were carried out at different temperatures in the range of 298-338K, in the absence and presence of 5×10^{-5} M of inhibitor (Figure 6). The obtained corrosion parameters are given in Table II which show that when temperature increases,

Table III Thermodynamic parameters for mild steel in 1.0 M HCl in the absence and presence of 5×10^{-5} M NKD

	E_a (kJmol^{-1})	ΔH°_{ads} (kJmol^{-1})	ΔS°_{ads} (Jmol^{-1}K^{-1})	ΔG°_{ads} (kJ mol^{-1})
HCl	21.3	−19.5	−277.7	–
NKD + HCl	56.54	−65.44	−275.5	−39.89

in absence and presence of inhibitor, j_{corr} increases. Based on Arrhenius equation, the logarithm of the corrosion rate ($\ln j_{corr}$) is a linear function with 1/T for the acid corrosion of steel (Li *et al.*, 2011):

$$\ln\ (j_{corr}) = -(E_a/RT) + \ln\ A \quad (8)$$

where E_a and A represent apparent activation energy and pre-exponential factor, respectively.

Arrhenius plot of $\ln j_{corr}$ vs 1/T for the blank acid solutions containing 5×10^{-5}M NKD inhibitor is shown in Figure 7, and the E_a values were calculated and the results are shown in Table III. The E_a value in absence of NKD is less than in its presence (Table III). This indicates that steel dissolution in presence of inhibitor is reduced by forming the iron-inhibitor complex.

The enthalpy of activation (ΔH°_{ads}) and the entropy change of activation (ΔS°_{ads}) for corrosion of steel in 1.0 M HCl in

Figure 6 Potentiodynamic curves for steel corrosion in 1.0 M HCl and 5×10^{-5} M NKD at different temperatures

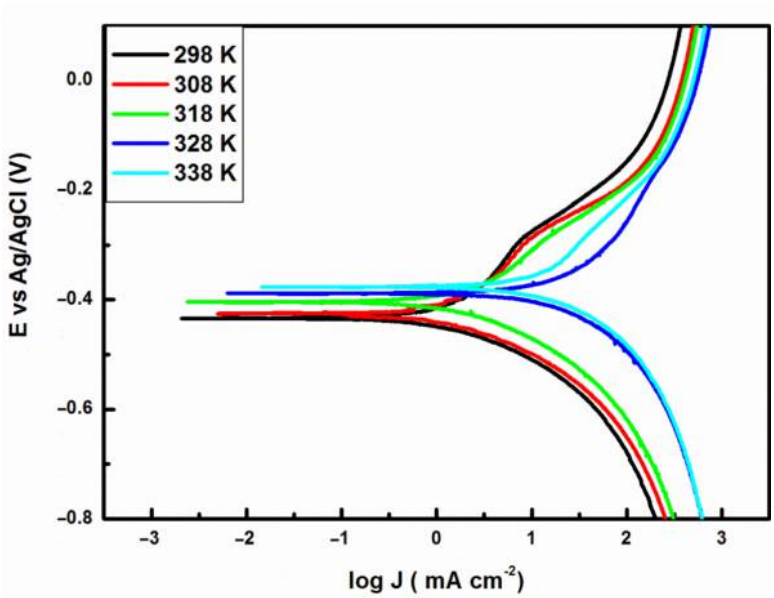

Figure 7 Arrhenius plots for the corrosion rate of steel in 1.0 M HCl in absence and presence of 5×10^{-5} M NKD

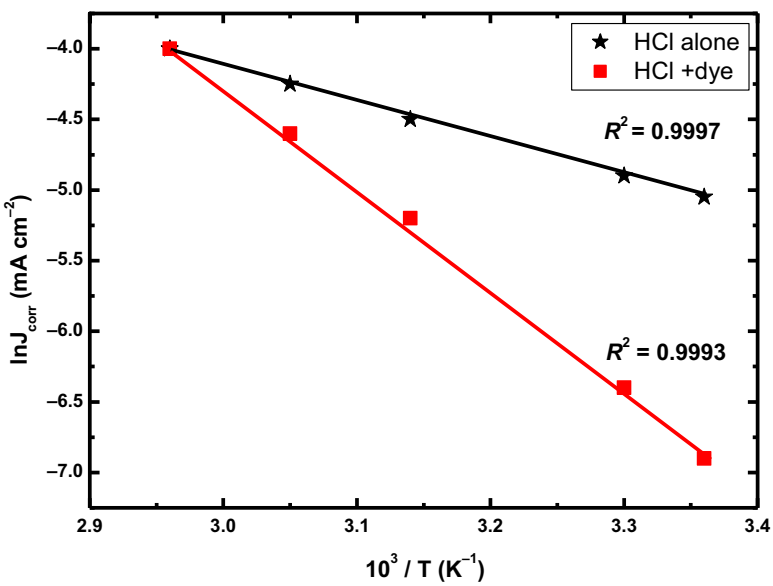

absence and presence of 5 × 10^{-5}M of the inhibitor are calculated using the following equation (Martinez, 2002).

$$\ln\left(\frac{j_{corr}}{T}\right) = ln\frac{R}{Nh} + \frac{\Delta S^{\circ}\ ads}{R} + \left(-\frac{\Delta H^{\circ} ads}{R}\right)\frac{1}{T} \quad (9)$$

Where h is Planck's constant, N is the Avogadro's number, ΔS°_{ads} is the entropy of activation. Figure 8 shows a plot of ln (j_{corr}/T) vs (1/T). Straight lines are obtained with a slope equal ($-\Delta H^{\circ}_{ads}/R$) and an intercept equal (ln R/Nh + $\Delta S^{\circ}_{ads}/R$) from which the values of ΔH°_{ads} and ΔS°_{ads} are calculated and listed in Table III. The negative sign of ΔH°_{ads} suggests that the adsorption of NKD on mild steel surface is an exothermic process, which means that the inhibition efficiency decrease as the temperature increases. This behavior can be explained on the bases that rising temperature leads to the desorption of some adsorbed inhibitor molecules from the steel surface. The values of ΔS°_{ads} in absence and presence of the studied inhibitor are large and negative. This indicates that the activated complex in the rate determining step represents an association rather than dissociation step, meaning that a decrease in disordering occurs from reactants to the activated complex (Quraishi and Khan, 2006).

3.5 UV-visible spectra

UV-visible absorption spectra obtained for 1.0 M HCl solution containing 5 × 10^{-4} M NKD before and after the steel immersion is carried out to confirm the possibility of the formation of inhibitor-Fe complex as shown in Figure 9. The electronic absorption spectra of NKD before immersion have absorption maximum at 415 and 585 nm, which can be attributed to π- $\pi^{\star}$ and n- $\pi^{\star}$ transitions. However, a decrease in the absorbance was observed after immersion of steel in HCl solution containing NKD for 4 h. Moreover, there is no change in the shape of the absorption spectra. These findings confirm the formation of complex between Fe^{2+} and NKD and consequently the inhibition of steel from corrosion.

3.6 Scanning electron microscopy analysis

SEM photomicrographs obtained for steel specimens immersed in 1.0 M HCl solution for 4 hours in the absence and presence of 5 × 10^{-5}M of NKD are shown in Figure 10(a,b). It can be observed from Figure 10(a) that the surface of the specimen in absence of NKD was greatly suffer from corrosion as observed by the presence of deep cracks on the surface. However, addition of NKD shows great improvement in the surface protection of the steel specimen due to the presence of adsorbed film on the surface which is responsible for the inhibition of corrosion as shown in Figure 10(b).

3.7 Quantum chemical calculations

The DFT has been used to predict the features of the inhibitor/surface mechanism and to outline the structural nature of the inhibitor on the corrosion process. In the present work, the quantum chemical study has been carried out with the help of DFT/B3LYP methods using 6–311 G (d, p) basis set because they are quite reliable for geometrical optimizations using Gaussian 09 program package (Frisch *et al.*, 2009).

The positions of atoms were correctly checked by examination of all possible free rotations to achieve a global minimum which is further confirmed by a frequency calculation. The structure of NKD has symmetrical bond lengths due to possessing C1 point group. The natural bond order atomic charges are shown in Figure 11 which shows the optimized geometry of NKD. The most negative atom is the oxygen atom of the hydroxyl group (0.401) followed by the aromatic carbons in ring (-0.010-0.394). Atomic charges suggest the opportunity of interaction between aromatic carbons and steel. The atom with the highest negative partial charge is considered a possible site for an attack by electron deficient species. On the other hand, the bond lengths (Figure 11) are located between 0.962 and 1.512 Ð indicating short bond lengths, which is correlated to chemisorption, while the physical interactions are associated with the bond lengths longer than 3.5 A° (Xie *et al.*, 2015).

Figure 8 Plots of ln (j_{corr}/T) versus 1/T for steel in 1.0 M HCl in absence and presence of 5 × 10^{-5} M NKD

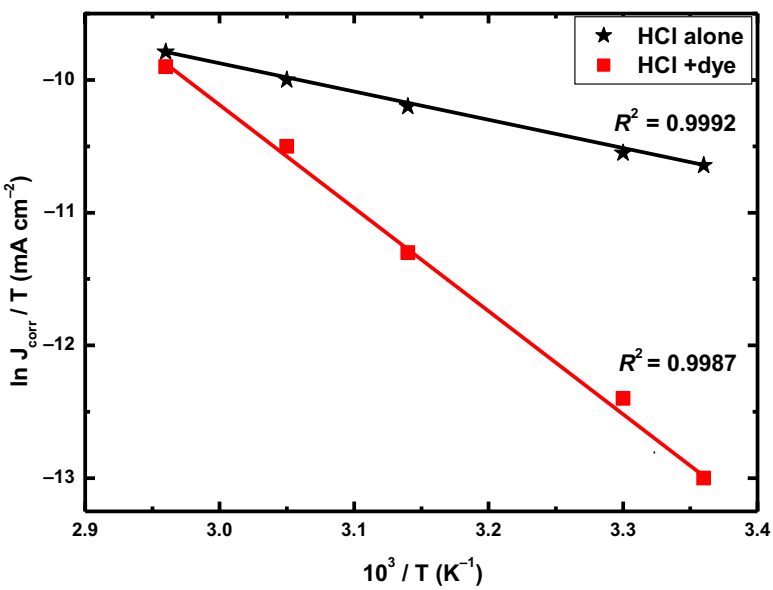

Figure 9 The SEM of steel specimens in 1.0 M HCl (a) in absence and (b) presence of NKD

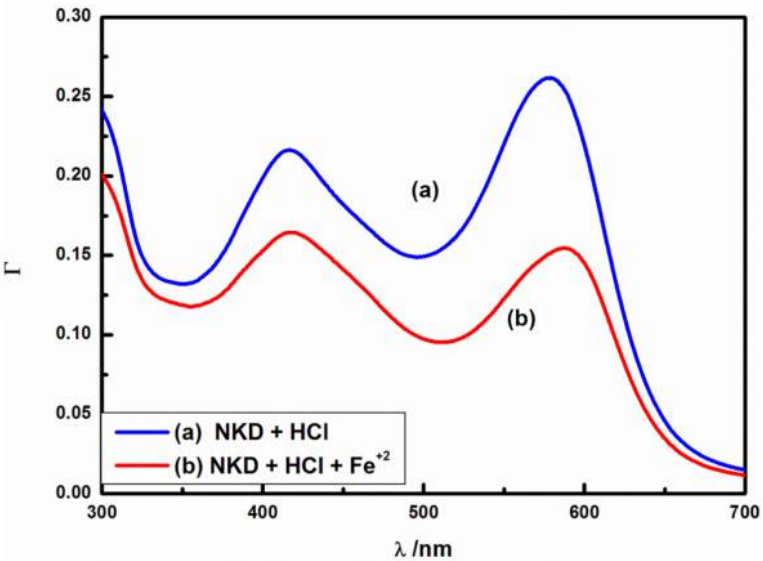

Figure 10 UV-visible for (a) 5×10^{-5} M NKD in 1.0 M HCl and (b) 5×10^{-5} M NKD in 1.0 M HCl containing Fe^{2+}

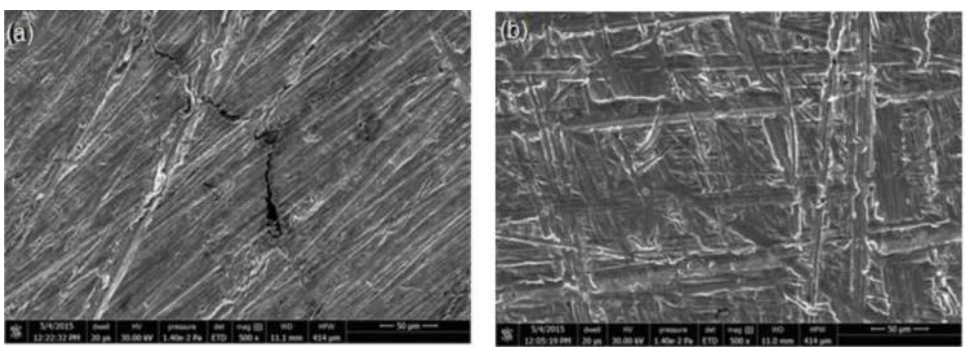

Figure 11 The optimized geometry of NKD (bond lengths in Å) and natural bond orbital atomic charges

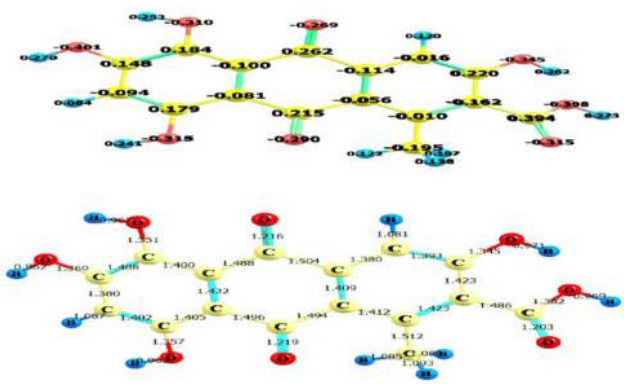

According to DFT, activity of inhibitor molecule is related to parameters that are assumed to have direct effect on interaction between inhibitor molecule and metal surface, i.e. E_{HOMO} often associated with the electron donating ability of the molecule to the empty molecular orbital of iron with low energy, and so the adsorption ability of this compound increases, and the inhibition efficiency increases with increasing E_{HOMO} values. Therefore, E_{LUMO} shows the ability of compound to accept electrons, and decrease in its value facilitates the ability of inhibitor molecule to accept an electron from metal surface (Cao *et al.*, 2014). For NKD, the molecular orbital plot of HOMO and LUMO are shown in Figure 12. The inhibition efficiency of the inhibitor can be evaluated by the orbital energy difference (ΔE). The smaller ΔE between the HOMO and LUMO, the stronger adsorption of the inhibitor molecules over the metal surface and consequently, the higher the inhibition efficiency (Mousavi *et al.*, 2011). The data listed in Table IV verified that NKD has high value of E_{HOMO} and low value of E_{LUMO} with low ΔE which supports its inhibition action on steel surface. Furthermore, the dipole moment μ is a measure of the polarity of a covalent bond, which is related to the distribution of electrons in a molecule. Generally, it is agreed that the large values of μ favor the adsorption of inhibitor onto a metal surface.

Figure 12 The molecular orbital plots of (a) HOMO and (b) LUMO

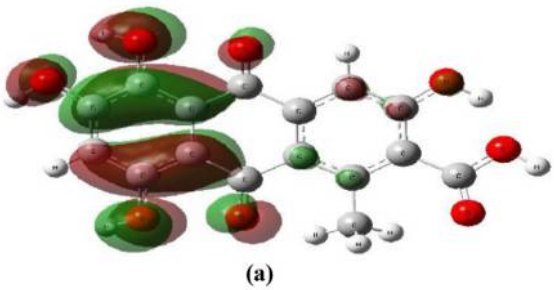

Table IV Molecular properties of NKD calculated using DFT at the B3LYP/6-311 G (p,d) basis set

Ground state properties	NKD
Total energy, E_T (au)	−1217.85
E_{HOMO} (eV)	−6.058256
E_{LUMO} (eV)	−2.648736
ΔE (eV) = $E_{LUMO} - E_{HOMO}$	3.40952
Dipole moment, μ (Debye)	5.4569
Ionization potential, I (eV) = −EHOMO	6.058256
Electron affinity, A (eV) = $-E_{LUMO}$	2.648736
Electronegativity, χ (eV)	4.353496
Global hardness, η (eV)	1.70476
Fractions of electron transfer, ΔN	1.13021657
E_{ads} (kcal/mol)	23.6

On the other hand, the fraction of electrons transferred from inhibitor molecule to the metallic atom (ΔN) was also calculated in the present study according to the following equation and the data are given in Table IV:

$$\Delta N = (\chi_{Fe} - \chi_{inh})/2(\eta_{Fe} + \eta_{inh}) \quad (10)$$

Where χ is the electronegativity (χ = I + A/2); I is the ionization potential (I = $-E_{HOMO}$) and η is the hardness (η = I − A/2). Increase in hardness increases the movement of the system toward a more stable configuration. Considering that χ_{Fe} = 7 eV and η_{Fe} = 0, and by assuming that for a metallic bulk I = A, ΔN can be calculated using equation (10). In the present study, it is found that ΔN are positive values (ΔN > 0) indicating that the inhibitor is donor of electrons. Furthermore, it indicates that the inhibitor retard corrosion by formation of an inhibitive layer. Therefore, this could be used as another method to correlate quantum parameters with inhibition efficiency. Generally, inhibition efficiency increases as the value of ΔN increases (Zhao *et al.*, 2005).

The optimized unit cell of steel is a body centered cube which is shown in Figure 13(a). The distance between Fe atom in the center and Fe atoms at the corners is 2.085 Å and the edge distance is 2.408 Å. Multiple of the unit cell were used to calculate the adsorption energy. The optimized geometry of the adsorbed NKD on steel is shown in Figure 13(b). The NKD inhibitor studied here is organic bases which can be protonated in acid medium, at the oxygen atoms. Thus, it becomes cation, the inhibitor cation adsorbed on the metal surface and releases protons. The overall process is shown in reaction (12) (Ahmad and Hassan, 2012).

$$\text{Inhibitor molecule} + H^+ \rightarrow \text{inhibitorcation} \quad (11)$$

$$\text{Inhibitorcation} + \text{Steel} \rightarrow \text{Inhibitor} - \text{Steel} + H^+ \quad (12)$$

$$\text{Inhibitormolecule} + \text{Steel} \rightarrow \text{Inhibitor} - \text{Steel} \quad (13)$$

Therefore, the interaction energy between the inhibitor molecule and the metal surface, E_{ads}, is the sum of the energies of steps (11) and (12) and can be calculated using equation (14):

$$E_{ads} = E_{inhibitor-steel} - (E_{inhibitor} + E_{steel}) \quad (14)$$

Where $E_{inhibitor-steel}$, $E_{inhibitor}$ and E_{steel} are electronic energies of the inhibitor–steel system, the inhibitor compound and the steel cluster, respectively. The value of E_{ads} is shown in Table IV. The high value of E_{ads} suggests that the adsorption of the NKD occurs via many centers. Figure 13(b) shows that many sites of interaction exist between NKD and steel mainly on the quinoline ring of the NKD molecule. Molecular dynamic simulations revealed a nearly flat configuration for molecules on metal surface with negative binding energies.

4. Conclusions

NKD acts effectively as an excellent corrosion inhibitor of steel in 1.0 M HCl as indicated from the impedance and potentiodynamic measurements. The IE% increases with increasing concentration and decreases with increasing temperature. The studied NKD acts as a mixed-type inhibitor. The adsorption of the studied NKD on steel surface obeys the Langmuir adsorption isotherm and involves chemical adsorption mechanism. The thermodynamic parameters of adsorption of NKD are calculated from their adsorption isotherm. Results obtained from UV-visible and SEM analyses confirmed the successful action of NKD as a corrosion inhibitor for steel in 1.0 M HCl. Theoretical data obtained from computational study are in good correlation with experimental data. We conclude that NKD may have the potential to replace toxic and expansive inhibitors.

Figure 13 The optimized geometry of (a) steel unit cell and (b) adsorbed NKD on steel

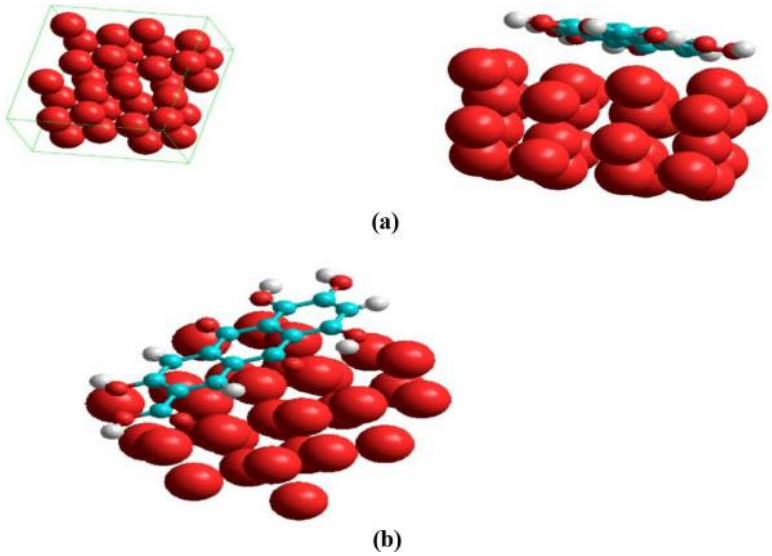

References

Abd El-Maksoud, S.A. and Hassan, H.H. (2007), "Electrochemical studies on the effect of (2E)-3-amino-2-phenylazo- but- 2- enenitrile and its derivative on the behavior of copper in nitric acid", *Materials Corrosion*, Vol. 58 No. 5, pp. 369-375.

Abdel-Gabar, A.M., Abd-El-Nabey, B.A., Sidahmed, I.M., El-Zayady, A.M. and Saadawy, M. (2006), "The corrosion inhibition of mild steel by ascorbic and folic acids", *Corrosion Science*, Vol. 28, pp. 987-1001.

Ahmad, Y.H. and Hassan, W.M.I. (2012), "Corrosion inhibition of steel in hydrochloric acid solution using a triazole derivative: electrochemical and computational studies", *International Journal of Electrochemical Science*, Vol. 7, pp. 12456-12469.

Ashassi-Sorkhabi, H. and Asghari, E. (2008), "Effect of hydrodynamic conditions on the inhibition performance of L-methionine as a green inhibitor", *Electrochimica Acta*, Vol. 54 No. 2, pp. 162-167.

Bacskay, G.B.A. (1981), "Quadratically convergent Hartree–Fock (QC-SCF) method"

Becke, A. (1993), "Density functional thermochemistry. III. the role of exact exchange", *Journal of Chemical Physics*, Vol. 98 No. 7, pp. 5648-5652, b) Becke, A. (1993), "Density functional thermochemistry. III. The role of exact exchange", *Journal of Chemical Physics*, Vol. 98, pp. 1372-1376.

Cao, K., Sun, H., Zhao, X. and Hou, B. (2014), "Investigation of novel Gemini surfactant with long chain alkyl ammonium head groups as corrosion inhibitor for copper in 3.5% NaCl", *International Journal of Electrochemical Science*, Vol. 9, pp. 8106-8119.

Dennington, R.K. Millam, T. and Semichem, J. (2009), GaussView, Version 5; Shawnee Mission KS.

Frisch, M. *et al.* (2009), Gaussian, Wallingford CT.

Hleli, S., Abdelghani, A. and Tlili, A. (2003), "Impedance spectroscopy technique for DNA hybridization", *Sensors*, Vol. 3 No. 10, pp. 472-479.

Hsu, C.S. and Mansfel, F. (2001), "Concerning the conversion of the constant phase element parameter Y0 into a capacitance", *Corrosion*, Vol. 57 No. 9, pp. 747-748.

Lebrini, M., Lagrenee, M., Vezin, H., Traisnel, M. and Bentiss, F. (2007), "Experimental and theoretical study for corrosion inhibition of mild steel in normal hydrochloric acid solution by some new macrocyclic polyether compounds", *Corrosion Science*, Vol. 49 No. 5, pp. 2254-2269.

Lee, C., Yang, W. and Parr, R.G. (1988), "Development of the Colle-Salvetti correlation-energy formula into a functional of the electron density", *Physical Review B*, Vol. 37 No. 2, pp. 785-789.

Li, X.H., Fu, H. and Deng, S.D. (2011), "Inhibition effect of dendrocalamus brandisii leaves extract on steel in hydrochloric acid solution", *Journal of the Chinese Society of Corrosion and Protection*, Vol. 21, pp. 149-154.

Liu, F.G., Du, M., Zhang, J. and Qiu, M. (2009), "Electrochemical behavior of Q235 steel in saltwater saturated with carbon dioxide based on new imidazoline derivative inhibitor", *Corrosion Science*, Vol. 51 No. 1, pp. 102-109.

Macdonald, J.R. and Johanson, W.B. (1987), in Macdonald, JR (Ed.). *Theory in Impedance Spectroscopy*, John Wiley & Sons, New York, NY.

Machnikova, E., Whitmire, K.H. and Hackerman, N. (2008), "Corrosion inhibition of carbon steel in hydrochloric acid by furan derivatives", *Electrochimica Acta*, Vol. 53 No. 20, p. 6024.

Martinez, S. (2002), "Thermodynamic characterization of metal dissolution and inhibitor adsorption processes in the low carbon steel/mimosa tannin/sulfuric acid system", *Applied Surface Science*, Vol. 199 Nos 1/4, pp. 83-99.

Matad, P.B., Mokshanatha, P.B., Hebbar, N., Venkatesha, V.T. and Tandon, H.C. (2014), "Ketosulfone drug as a green corrosion inhibitor for mild steel in acidic medium", *Industrial & Engineering Chemistry Research*, Vol. 53 No. 20, pp. 8436-8444.

Mousavi, M., Mohammadalizadeh, M. and Khosravan, A. (2011), "Theoretical investigation of corrosion inhibition effect of imidazole and its derivatives on mild steel using cluster model", *Corrosion Science*, Vol. 53 No. 10, pp. 3086-3091.

Musa, A.Y., Kadhum, A.A.H., Mohamad, A.B., Daud, A.R., Takriff, M.S. and Kamarudin, S.K. (2009), "A comparative study of the corrosion inhibition of mild steel in sulphuric acid by 4,4-dimethyloxazolidine-2-thione", *Corrosion Science*, Vol. 51 No. 10, pp. 2393-2399.

Oguzie, E.E. (2004), "Influence of halide ions on the inhibitive effect of Congo red dye on the corrosion of mild steel in sulphuric acid solution", *Materials Chemistry and Physics*, Vol. 87 No. 1, pp. 12-217.

Oguzie, E.E., Okolue, B.N., Ogukwe, C.E. and Unaegbu, C. (2006), "Corrosion inhibition and adsorption of bismark brown dye on aluminium in sodium hydroxide solution", *Materials Letters*, Vol. 60 No. 28, pp. 3376-3378.

Oguzie, E.E., Unaegbu, C., Ogukwe, C.E., Okolue, B.N. and Onuchukwu, A.I. (2004a), "Inhibition of mild steel corrosion in sulphuric acid using indigo dye and synergistic halide additives", *Materials Chemistry and Physics*, Vol. 84 Nos 2/3, pp. 363-368.

Oguzie, E.E., Okolue, B.N., Ebenso, E.E., Onuoha, G.N. and Onuchukwu, A.I. (2004b), "Evaluation of the inhibitory effect of methylene blue dye on the corrosion of aluminium in hydrochloric acid", *Materials Chemistry and Physics*, Vol. 87 Nos 2/3, pp. 394-401.

Olasunkanmi, L.O., Obot, V., Kabanda, M.M. and Ebenso, E. E. (2015), "Some quinoxalin-6-yl derivatives ascorrosion inhibitors for mild steel in hydrochloric acid: experimental and theoretical studies", *The Journal of Physical Chemistry C*, Vol. 119 No. 28, pp. 16004-16019.

Quraishi, M.A. and Khan, S. (2006), "Inhibition of mild steel corrosion in sulfuric acid solution by thiadiazoles", *Journal of Applied Electrochemistry*, Vol. 36 No. 5, pp. 539-544.

Quraishi, M.A. and Rawat, J. (2002), "Corrosion inhibiting action of tetramethyl-dithia-octaaza-cyclotetradeca-hexaene (MTAH) on corrosion of mild steel in hot 20% sulfuric acid", *Materials Chemistry and Physics*, Vol. 77 No. 1, pp. 43-47.

Saliyan, V.R. and Adhikari, A.V. (2008), "Quinolin-5-ylmethylene-3-{{[8-(trifluoromethyl)quinolin-4-yl]thio}propanohydrazide as an effective inhibitor of mild steel corrosion in HCl solution", *Corrosion Science*, Vol. 50, pp. 55-61.

Sekine, I., Nakata, Y. and Tanabe, H. (1988), "The corrosion inhibition of mild steel by ascorbic and folic acids", *Corrosion Science*, Vol. 28 No. 10, pp. 987-1001.

Sorkhabi, H.A., Shaabani, B. and Seifzadeh, D. (2005), "Corrosion inhibition of mild steel by some schiff base compounds in hydrochloric acid", *Applied Surface Science*, Vol. 239 No. 2, pp. 154-164.

Stefanov, B. Liu, B.G. Liashenko, A. Piskorz, P. Komaromi, I. Martin, R.L. Fox, D.J. Keith, T. Al-Laham, M.A. Peng, C. Y. Nanayakkara, A. Challacombe, M. Gill, P.M.W. Johnson, B. Chen, W. Wong, M.W. Gonzalez, C. and Pople, J.A. (2003), Gaussian, Pittsburgh PA.

Stewart, J.J.P. (2007), "Optimization of parameters for semiempirical methods V: modification of NDDO approximations and application to 70 elements", *Journal of Molecular Modeling*, Vol. 13 No. 12, pp. 1173-1213.

Ulaeto, S.B., Ekpe, U.J., Chidiebere, M.A. and Oguzie, E.E. (2012), "Corrosion inhibition of mild steel in HCl by acid extract of eichhornia crassipes", *International Journal of Material Chemistry*, Vol. 2, pp. 158-164.

Wang, Z. (2012), "The inhibition effect of bis-benzimidazole compound for mild steel in 0.5 M HCl solution", *International Journal of Electrochemical Science*, Vol. 7, pp. 11149-11160.

Xie, S.W., Liu, Z., Han, G.C., Li, W., Liu, J. and Chen, Z. (2015), "Molecular dynamics simulation of inhibition mechanism of 3,5-dibromo salicylaldehyde Schiff's base", *Computational and Theoretical Chemistry*, Vol. 1063, pp. 50-62.

Yan, Y., Li, Wh. and Cailk Hou, Br. (2008), "Electrochemical and quantum chemical study of purines as corrosion inhibitors for mild steel in 1M HCl solution", *Electrochimica Acta*, Vol. 53 No. 20, pp. 5953-5960.

Yurt, A., Bereket, G., Kivrak, A., Balaban, A. and Erk, B. (2005), "Effect of Schiff bases containing pyridyl group as corrosion inhibitors for low carbon steel in 0.1 M HCl", *Journal of Applied Electrochemistry*, Vol. 35 No. 10, pp. 1025-1032.

Zhao, P., Liang, Q. and Li, Y. (2005), "Electrochemical, SEM/EDS and quantum chemical study of phthalocyanines as corrosion inhibitors for mild steel in 1 mol/l HCl", *Applied Surface Science*, Vol. 252 No. 5, pp. 1596-1607.

Corresponding author

Magdy A.M. Ibrahim can be contacted at: imagdy1963@hotmail.com